Cement & Concrete Composites 32 (2010) 255–264

Contents lists available at ScienceDirect

Cement & Concrete Composites

journal homepage: www.elsevier.com/locate/cemconcomp

Role of water film thickness in rheology of CSF mortar

W.W.S. Fung, A.K.H. Kwan *

Department of Civil Engineering, The University of Hong Kong, Hong Kong, China

ARTICLE INFO

Article history:
Received 24 October 2009
Received in revised form 22 January 2010
Accepted 23 January 2010
Available online 1 February 2010

Keywords:
Condensed silica fume
Flowability
Mortar
Rheology

ABSTRACT

In a recent study, the authors have demonstrated that the combined effects of water content, packing density and solid surface area on the rheology of cement–sand mortar may be evaluated in terms of the water film thickness (WFT). The present study aims to extend the concept of WFT to mortar containing condensed silica fume (CSF). For the study, mortar samples with various CSF and water contents were made for packing density, flowability and rheology measurements. It was found that although the effects of adding CSF are fairly complicated, the WFT is still the single most important parameter governing the rheology of CSF mortar. However, the rheological properties are dependent also on the CSF content. Correlations of the rheological properties to both the WFT and CSF content yielded R^2 values of at least 0.896.

1. Introduction

The use of supplementary cementitious materials (SCM) in concrete offers great benefits. First, as the consumption of cement clinker would be lowered, the carbon footprint of the concrete production could be reduced, thus contributing to sustainable development. Second, some of the SCM are industrial by-products or wastes that are cheaper than cement. Their addition to replace part of the cement would render the concrete production more economical. Third and foremost, concrete produced with SCM added is often found to perform better in terms of strength, workability and durability [1–4]. Because of these benefits, the use of SCM has become more and more popular, especially in the production of high-strength concrete (HSC) and high-performance concrete (HPC).

Among the various types of SCM, condensed silica fume (CSF) has the greatest effects on the properties of concrete. It is a by-product of the production of silicon metal or ferrosilicon alloys [5]. Because of its high fineness and pozzolanic activity (the pozzolanic reaction is the chemical reaction between the silica in SCM and the lime in concrete), the addition of CSF can effectively increase the concrete strength. In fact, HSC with cube strength higher than 85 MPa was first commercially produced in 1980s by adding CSF [6]. Since then, CSF has become an indispensable ingredient for HSC. Due to the filling and pore refinement effects, the addition of CSF can greatly improve the durability of concrete structures. As reported by Hooton [7] and Bayasi and Zhou [8] in 1993, the permeability of CSF concrete decreases with increasing CSF content and is generally much lower than that of plain concrete with no CSF added. Likewise, Alexander and Magee [9] found in 1999 that compared to plain concrete, CSF concrete generally has lower gas permeability, water sorptivity and chloride conductivity, which all contribute to better durability. More recently, Mazloom et al. [10] showed in 2004 that the addition of CSF not only increases the strength but also reduces the creep of the concrete.

However, it has been found that the addition of CSF has very complicated effects, which may either be beneficial or detrimental, on the flowability of cement paste/mortar/concrete. In 1986, Kohno and Komatsu [11] reported that at the same water/binder ratio and superplasticizer (SP) dosage, a mortar containing CSF would have a smaller flow compared with a plain mortar containing no CSF. In 1998, Duval and Kadri [12] examined a number of concrete mixes with different CSF contents and found that the concrete mix with 10% CSF content by weight has the lowest required SP dosage for the same slump. Likewise, in 2000, Zhang and Han [13] showed that the yield stress and viscosity of a cement paste could be remarkably decreased if CSF is added to replace 10% by weight of cement. More recently, in 2008, Artelt and Garcia [14] examined several mortar mixes with and without CSF and concluded that the presence of CSF would impair the flowability as evidenced by the smaller flow spread and longer flow time obtained for the CSF mortars. Up to now, no general conclusion can be made on the effects of CSF on the flowability.

In theory, the addition of CSF should have two main effects on the flowability. On one hand, the ultrafine CSF particles would fill into the voids between cement grains to increase the packing

* Corresponding author. Tel.: +852 2859 2647; fax: +852 2559 5337.
E-mail addresses: wilsonf1@graduate.hku.hk (W.W.S. Fung), khkwan@hku.hk (A.K.H. Kwan).

0958-9465/$ - see front matter © 2010 Elsevier Ltd. All rights reserved.
doi:10.1016/j.cemconcomp.2010.01.005

density of the solid particles so that the amount of excess water (the amount of water in excess of that needed to fill up the voids) available for lubrication would be increased. On the other hand, due to the high fineness of CSF, the addition of CSF would markedly increase the surface area of the solid particles and thus for the same amount of excess water, the thickness of the water films coating the solid particles would be decreased. The increase in packing density and the increase in surface area have opposite effects on the flowability and therefore their net influence could be either positive or negative, depending on the relative magnitudes of such opposite effects. To evaluate these opposite effects so as to improve our understanding of the net influence of CSF, systematic studies on the packing density and water film thickness are needed.

The concepts of packing density and water film thickness are not new. Early in 1980, Helmuth [15] has suggested that it should be the thickness of the water films coating the cement grains that governs the consistence of cement paste. Similarly, in 1996, Zhang et al. [16] pointed out that the water in a cement paste may be divided into two portions: one portion is the filling water, which fills into the voids between the solid particles and does not contribute to the fluidity of the paste, while the other portion is the excess water, which forms a water film on the surface of each solid particle and contributes to the fluidity of the paste. In recent years, due to increasing usage of SCM in HSC and HPC, there appears to be an intensified interest in these concepts. For instance, in 2008, Nanthagopalan et al. [17] studied the effects of packing density on the flowability of cement paste and in 2009, Peng et al. [18] studied the effects of SCM on the packing density of cementitious materials. However, so far, there has been basically no research on how the water film thickness (WFT) would affect the flowability of cement paste, mortar and concrete.

Recently, the authors' research group has successfully developed a new wet packing test for direct measurement of the packing density of cementitious materials [19], fine aggregate [20] and cementitious materials plus fine aggregate [21], and with the use of existing packing models, verified the accuracy and applicability of this wet packing test [21,22]. With the packing density so directly measured and then the WFT determined as the excess water to solid surface area ratio, the authors' research group has demonstrated that the WFT should be the single most important parameter governing the flowability and rheological properties of cement paste [23,24] and cement–sand mortar [25]. Knowing that the addition of CSF would affect both the packing density and solid surface area, the authors are of the view that CSF might be exerting its influence mainly through its effects on the WFT, which in turn governs the flowability and rheology of cement paste/mortar/concrete.

In order to study the role of WFT in the flowability and rheology of CSF mortar and evaluate the effects of CSF, a comprehensive testing program was carried out, as reported herein. A total of 45 mortar samples with CSF contents varying from 0% to 25% by volume and different water contents were made for packing density and rheology measurements. Each mortar sample represented the mortar portion of a concrete mix. The packing density of each mix of solid particles was measured using the wet packing test recently developed by the authors' research group while the WFT of each mortar sample was determined as the excess water to solid surface area ratio. At the same time, for each mortar sample, the flowability was measured in terms of flow spread and flow rate, and the rheological properties were measured in terms of yield stress and apparent viscosity. These results were then correlated to the WFT for in-depth analysis of the combined effects of WFT and CSF content.

2. Determination of water film thickness

To determine the WFT of a mortar sample, it is necessary first of all to measure the packing density of the solid particles in the mortar. From the packing density of the solid particles τ (defined as the ratio of the solid volume to the bulk volume of the particles), the voids ratio of the solid particles u (defined as the ratio of the voids volume to the solid volume of the particles) can be evaluated as:

$$u = \frac{1-\tau}{\tau} \tag{1}$$

Having evaluated the above voids ratio, the excess water ratio of the mortar u'_w (defined as the ratio of the volume of excess water to the solid volume of the particles) can be obtained as:

$$u'_w = u_w - u \tag{2}$$

where u_w is the water ratio of the mortar (defined as the ratio of the volume of water to the solid volume of the particles). At the same time, the specific surface area of the solid particles (defined as the solid surface area per unit solid volume) in the mortar A_M can be calculated as:

$$A_M = A_C \times R_C + A_{CSF} \times R_{CSF} + A_{FA} \times R_{FA} \tag{3}$$

in which A_C, A_{CSF} and A_{FA} are respectively the specific surface areas of cement, CSF and fine aggregate, and R_C, R_{CSF} and R_{FA} are respectively the volumetric ratios of cement, CSF and fine aggregate to the total solid volume. With the values of u'_w and A_M so determined, the WFT, which has the physical meaning of being the average thickness of the water films coating the solid particles, may be obtained as:

$$\mathrm{WFT} = \frac{u'_w}{A_M} \tag{4}$$

3. Experimental program

To study the role of WFT in the flowability and rheology of CSF mortar, an experimental program was carried out, in which mortar mixes containing different amounts of CSF were made for examination. Six different CSF contents, namely, 0%, 5%, 10%, 15%, 20% and 25% by volume of the total cementitious materials, were adopted for the design of the mortar mixes. To exclude the effect of fine aggregate, the ratio of total cementitious materials to fine aggregate was fixed at 0.75 by volume. At the same time, the water/solid (W/S) ratio by volume was varied in steps of 0.05 from 0.35 to 0.65 for CSF contents of 0%, 5% and 10% and from 0.35 to 0.70 for CSF contents of 15%, 20% and 25%. A SP was added to each mortar sample at a dosage of 93.3 kg/m^3 by liquid mass of the SP to the solid volume of the cementitious materials (equivalent to 3% by mass of cement when only cement is added as cementitious material), which is the maximum dosage recommended by the supplier. The high SP dosage was to minimize agglomeration of the CSF particles. For easy identification, each mortar sample is assigned a designation of *X*–*Y*, where *X* denotes the CSF content (A = 0%, B = 5%, C = 10%, D = 15%, E = 20% and F = 25%) and *Y* denotes the W/S ratio.

Each mortar sample was produced by mixing the ingredients in a standard mixer complying with BS EN 196: Parts 1–3. To ensure thorough mixing of the cementitious materials and fine aggregate with water, a special mixing procedure of adding the solid materials in several small increments to the water was adopted. The authors' research group has been using this method of mixing in previous studies [19,23,24] because the conventional method of mixing all the solid materials with water in a single batch would encounter difficulties when the water content is low and/or the CSF content is high due to the apparent dryness of the mixture formed. The whole sample preparation and testing procedures

were carried out in a laboratory maintained at a temperature of 24 ± 2 °C.

3.1. Materials

An ordinary Portland cement (OPC) of strength class 52.5 N and a condensed silica fume (CSF) were used as the only cementitious materials. The OPC used was obtained from the local market and had been tested to comply with BS 812: 1996 while the CSF used was imported from Norway and had been tested by the supplier to comply with ASTM C 1240-03. As for the fine aggregate, local crushed granite rock fine with a maximum size of 1.18 mm and a water absorption of 1.6% by mass was used. The relative densities of the OPC, CSF and fine aggregate had been measured in accordance with BS 812: Part 2: 1995 as 3.11, 2.20 and 2.66, respectively, whereas the Blaine fineness of the OPC had been measured in accordance with BSEN 196-6: 1992 as 345 m^2/kg. A laser diffraction particle size analyzer was used to measure the particle size distributions of the materials and the results are plotted in Fig. 1. Based on these particle size distributions, the specific surface areas of the OPC, CSF and fine aggregate were calculated to be 1.40×10^6, 1.33×10^7 and 2.10×10^5 m^2/m^3, respectively. The SP employed was a polycarboxylate-based type with a solid mass content of 20% and a relative density of 1.03.

3.2. Measuring flow spread and flow rate

The mini slump cone test and mini V-funnel test were used to measure the flow spread and flow rate, respectively, of the mortar samples. Both the mini slump cone and mini V-funnel tests for mortar may be regarded as reduced scale versions of the slump and V-funnel tests for concrete.

There are several versions of mini slump cone test employing slump cones of different dimensions. The version adopted herein is the same as that used by Okamura and Ouchi [26], which employs a slump cone of dimensions as shown in Fig. 2a. The test procedures are detailed in the following:

(i) Place the slump cone at the centre of a flat, smooth and level steel plate.
(ii) Pour the mortar into the slump cone until the slump cone is completely filled up and trowel flat the top surface of the mortar with a straight edge.
(iii) Lift the slump cone gently and allow the mortar to flow and spread for at least 3 min.

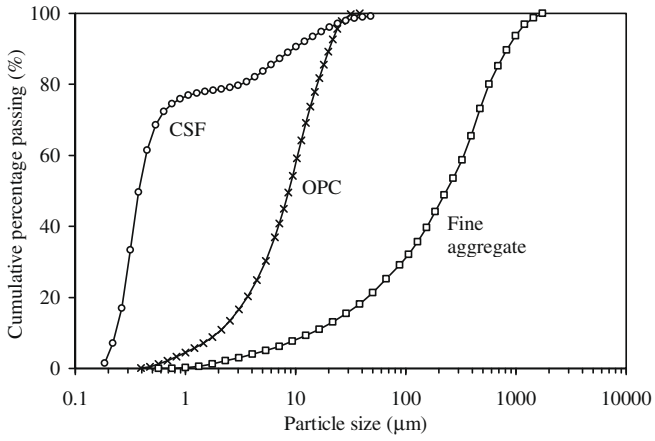

Fig. 1. Particle size distributions of OPC, CSF and fine aggregate.

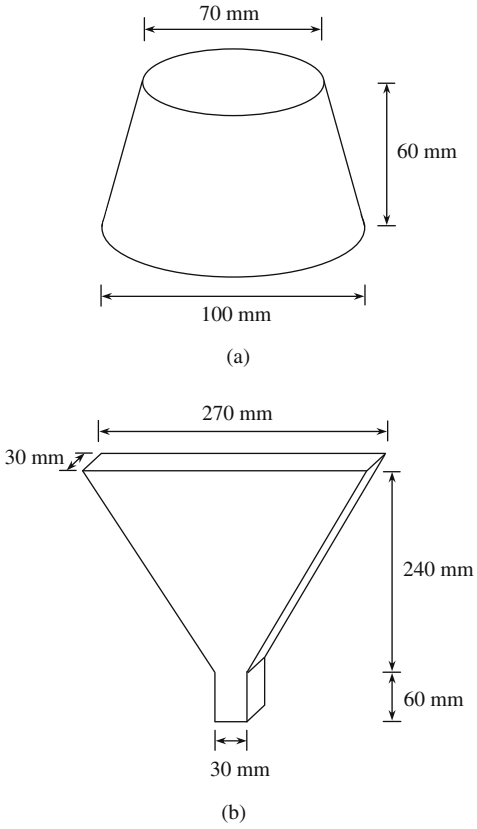

Fig. 2. (a) Mini slump cone and (b) mini V-funnel.

(iv) Measure two perpendicular diameters of the mortar patty formed, calculate the average diameter and determine the flow spread of the mortar as the average diameter minus the base diameter of the slump cone.

Likewise, there are several versions of mini V-funnel test employing V-funnels of different dimensions. The version adopted herein is the same as that used by Okamura and Ouchi [26], which employs the V-funnel of dimensions as shown in Fig. 2b. The test procedures are detailed in the following:

(i) Mount the V-funnel on a stable stand and close the opening of the V-funnel at the bottom.
(ii) Pour the mortar into the V-funnel until the V-funnel is completely filled up. To minimize air entrapment, pour the mortar slowly along the inner surfaces of the V-funnel.
(iii) Open the opening of the V-funnel to let the mortar flow out. Record the time from the start of the flow to the first sight of light through the opening. The recorded time is the flow time of the mortar. Calculate the flow rate as the volume of mortar sample (equal to 1134 ml) divided by the flow time.

3.3. Measuring rheological properties

The vane test was used to evaluate the rheological properties of the mortar samples. It was carried out using a speed-controlled rheometer equipped with a shear vane, measuring 20 mm in width and 40 mm in length, and a cylindrical container, having an inner diameter of 40 mm, as shown in Fig. 3. The inner wall of the container was profiled with grooves in such a way that the asperity was larger than the largest particle in the mortar sample being

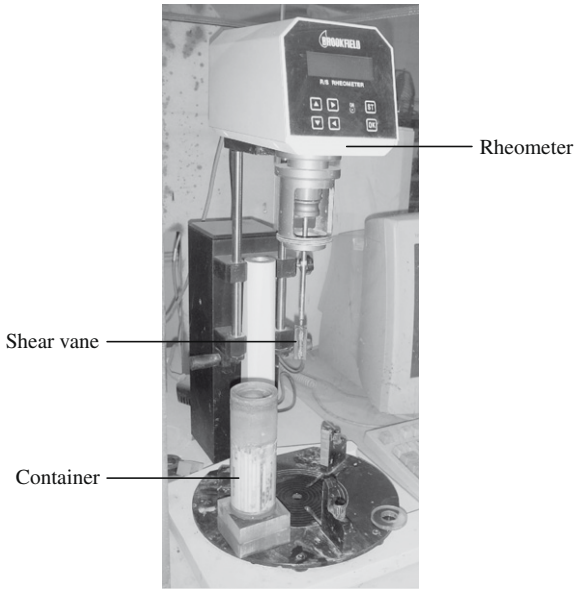

Fig. 3. Rheometer, shear vane and container.

tested. This was to minimize slippage of the mortar at the container surface during shearing.

At the onset of the test, the shear vane was concentrically inserted into the mortar sample in the cylindrical container and then set to rotate at controlled rotation speed, following a shearing sequence which consisted of two shearing cycles. The first cycle, called the pre-shearing cycle, was to apply pre-shearing to the sample so that all the samples tested had the same shearing history before measurement. The second cycle, called the data-logging cycle, was for the actual measurement. In the data-logging cycle, the rotation speed N (measured in terms of rpm, i.e. rotation per minute) was increased from 0 to 50 rpm in 75 s and then decreased to 0 rpm in another 75 s. During shearing, the torque T (measured in terms of mN m) induced at the shear vane was continuously monitored and regularly logged by a computer. The results obtained at decreasing rotation speed, which are generally more consistent and repeatable, were used for evaluating the rheological properties of the mortar sample.

As the mortar is non-Newtonian, it is customary to describe its rheological properties by either the Bingham model (which assumes that the shear stress–shear rate curve is linear) or the Herschel–Bulkley model (which assumes that the shear stress–shear rate curve follows the power equation). Upon curve fitting using both models, it was found that the experimental results agreed better with the Herschel–Bulkley model, whose shear stress–shear rate relation is given by:

$$\tau = \tau_0 + k\dot{\gamma}^n \tag{5}$$

where τ is shear stress (Pa), $\dot{\gamma}$ is shear rate (s^{-1}), τ_0 is yield stress (Pa), and k (Pa s^n) and n (non-dimensional) are empirical coefficients. To evaluate the rheological properties of the mortar sample tested, the best-fit curve based on the above equation was first obtained by regression analysis. Then, from the best-fit curve so obtained, the yield stress (taken as the shear stress at a shear rate of zero) and apparent viscosity (taken as the ratio of shear stress to shear rate at a shear rate of 14 s^{-1}) were determined to characterise the rheology of the mortar sample.

3.4. Measuring packing density

The wet packing test recently developed by the authors' research group for cementitious materials [19], fine aggregate [20] and cementitious materials plus fine aggregate [21] was used to measure the packing density of the solid particles (mixture of cementitious materials and fine aggregate) in the mortar. In principle, the wet packing test measures the solid concentrations of the mortar samples produced at different W/S ratios and determines the packing density of the solid particles under wet condition as the maximum solid concentration so obtained. Compared to the existing dry packing test for fine and coarse aggregates stipulated in BS 812: Part 2: 1995, this wet packing test has the overwhelming advantage that the effects of water and SP (if any) are incorporated because the packing density measurement is conducted with water and SP (if any) added.

Since the cementitious materials to fine aggregate ratio was fixed, the 45 mortar samples were actually made from six different mixes of cementitious materials and fine aggregate. The 6 mixes are numbered from A to F and have CSF contents of 0%, 5%, 10%, 15%, 20% and 25%, respectively. For each mix, 8–10 mortar samples were produced at different W/S ratios. The same SP at the same dosage of 93.3 kg/m^3 of the volume of cementitious materials was added to each mortar sample. After mixing by the same procedure as mentioned before, the solid concentrations of the mortar samples were measured and the maximum solid concentration so obtained was taken as the packing density of the mix of cementitious materials and fine aggregate.

4. Experimental results

4.1. Flow spread and flow rate

The flow spread and flow rate results of the mortar samples are tabulated in the second and third columns of Table 1, and plotted against the W/S ratio in Fig. 4. It is evident from the curves plotted in the figure that both the flow spread and flow rate increased with increasing W/S ratio. These observed phenomena are expected, as increasing the water content of a mortar should always improve the flowability. It is also noted that at the same W/S ratio, both the flow spread and flow rate varied with the CSF content. This is depicted by the different curves plotted for the mortar samples with different CSF contents. However, the variations of the flow spread and flow rate with the CSF content appeared to be quite complicated and dependent on the W/S ratio.

Close examination of the flow spread and flow rate results in Table 1 revealed that at a constant W/S ratio lower than 0.50, the flow spread and flow rate firstly increased when the CSF content was increased from 0% to about 5–15% and then decreased when the CSF content was further increased. Hence, at a relatively low W/S ratio, there are an optimum CSF content for maximum flow spread and an optimum CSF content for maximum flow rate. On the other hand, at a W/S ratio of 0.50 or higher, the flow spread changed only slightly when the CSF content was increased from 0% to 10% and then decreased steadily when the CSF content was further increased, while the flow rate decreased steadily right at the beginning when the CSF content was increased from 0% onwards.

4.2. Yield stress and apparent viscosity

The yield stress and apparent viscosity results of the mortar samples are tabulated in the fourth and fifth columns of Table 1, and plotted against the W/S ratio in Fig. 5. From the curves plotted, it can be seen that both these two rheological properties gradually decreased as the W/S ratio increased. This agrees with the general observation that increasing the water content of a mortar would reduce the yield stress and apparent viscosity. It can also be seen that at the same W/S ratio, both these rheological properties varied

Table 1
Flowability and rheological properties of the mortar samples.

Sample no.	Flow spread (mm)	Flow rate (ml/s)	Yield stress (Pa)	Apparent viscosity (Pa s)
A-0.35	204	48	14.12	22.52
A-0.40	272	127	4.24	7.08
A-0.45	286	188	2.86	4.85
A-0.50	288	275	2.09	2.52
A-0.55	294	350	1.00	2.02
A-0.60	295	450	0.95	1.15
A-0.65	298	603	0.85	0.50
B-0.35	231	71	9.20	14.50
B-0.40	276	142	3.83	6.03
B-0.45	293	202	2.30	3.99
B-0.50	296	263	1.64	2.87
B-0.55	295	318	0.73	2.26
B-0.60	293	387	0.54	1.07
B-0.65	288	511	0.50	0.99
C-0.35	230	82	7.83	13.30
C-0.40	280	151	2.75	5.60
C-0.45	297	210	1.51	3.89
C-0.50	297	255	1.20	2.94
C-0.55	302	312	0.93	2.02
C-0.60	300	374	0.92	1.87
C-0.65	302	431	0.90	1.35
D-0.35	225	88	8.25	12.30
D-0.40	265	142	2.59	6.58
D-0.45	287	189	1.93	4.32
D-0.50	290	252	1.12	3.08
D-0.55	291	292	0.50	2.45
D-0.60	291	359	0.50	2.43
D-0.65	292	391	0.47	1.57
D-0.70	285	471	0.40	1.31
E-0.35	193	76	9.44	14.56
E-0.40	240	133	5.00	6.88
E-0.45	270	175	2.90	5.10
E-0.50	278	224	2.07	3.58
E-0.55	278	284	1.36	2.92
E-0.60	280	330	0.89	2.29
E-0.65	280	363	0.60	1.89
E-0.70	280	426	0.48	1.70
F-0.35	195	66	8.30	16.11
F-0.40	222	125	4.35	7.91
F-0.45	249	170	2.39	5.10
F-0.50	269	216	1.81	3.69
F-0.55	269	257	1.61	3.01
F-0.60	274	312	1.55	2.50
F-0.65	274	374	1.27	2.36
F-0.70	274	412	1.10	2.04

Note: Sample codes A–F indicate CSF contents of 0%, 5%, 10%, 15%, 20% and 25%, respectively.

with the CSF content, as illustrated by the different curves plotted for the mortar samples with different CSF contents. Hence, it may be concluded that the rheological properties of a mortar are governed not just by the water content but also by the CSF content. As before, the variations of the rheological properties with the CSF content appeared to be quite complicated.

From the yield stress results in Table 1, it is seen that at all the W/S ratios covered in the present study, the yield stress first decreased when the CSF content was increased from 0% to about 5–15% and then increased when the CSF content was further increased. Hence, regardless of the W/S ratio, there is an optimum CSF content for minimum yield stress. On the other hand, from the apparent viscosity results in Table 1, it is also seen that at a W/S ratio lower than 0.50, the apparent viscosity first decreased when the CSF content was increased from 0% to about 5–15% and then increased when the CSF content was further increased. Hence, at a relatively low W/S ratio, there is an optimum CSF content for minimum apparent viscosity. However, at a W/S ratio of 0.50 or higher, the apparent viscosity increased steadily and slowly right

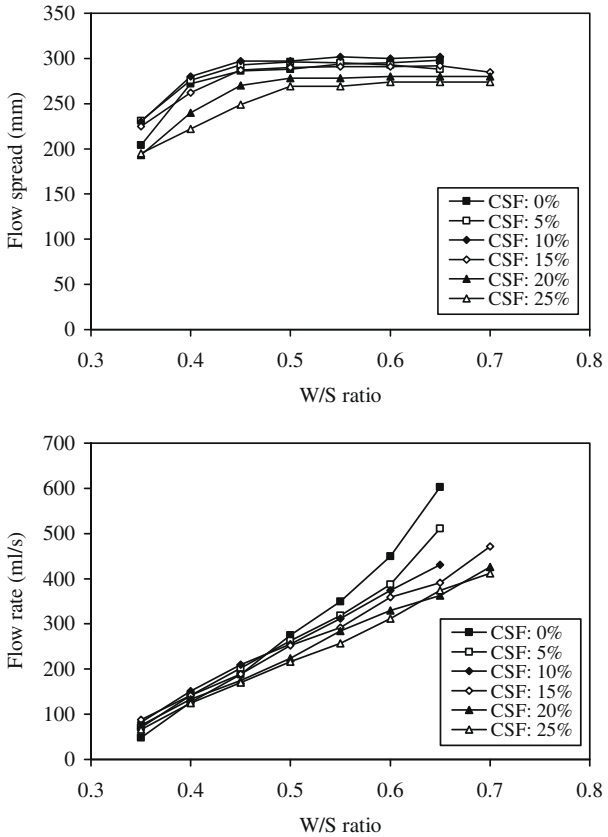

Fig. 4. Flowability versus W/S ratio.

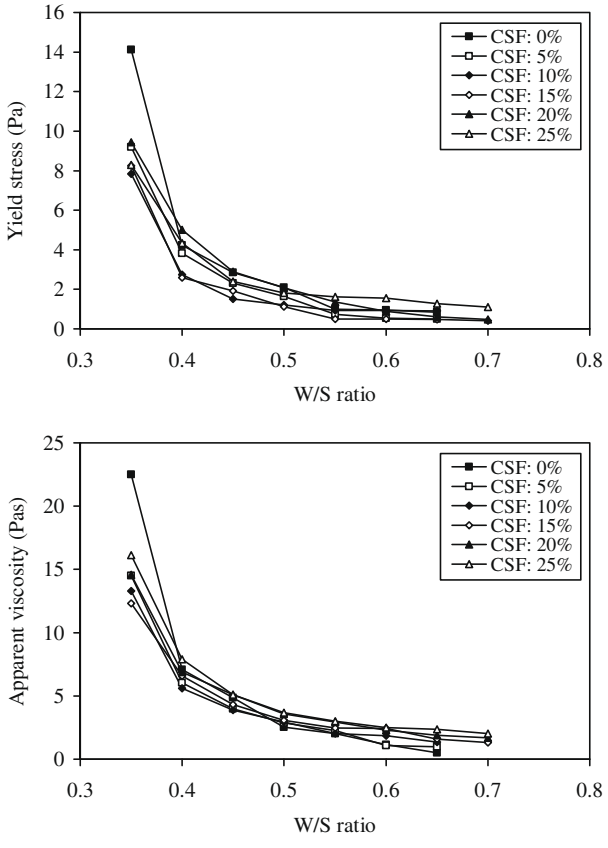

Fig. 5. Rheological properties versus W/S ratio.

at the beginning when the CSF content was increased from 0% onwards.

5. Roles of packing density and solid surface area

5.1. Packing density

All the mortar samples tested were actually made from six mixes of OPC, CSF and fine aggregate. The packing density results of these six mixes are tabulated in the second column of Table 2. From the packing density results, it can be seen that every mix containing CSF has a higher packing density than the one containing no CSF. This may be attributed to the filling effect of the CSF particles. Because of their very small size, the CSF particles filled themselves into the voids between the OPC and fine aggregate particles and thus increased the solid concentration of the mix of cementitious materials and fine aggregate. Furthermore, it can also be seen that the packing density increased almost linearly with the CSF content up to a CSF content of 25%. More specifically, with 25% CSF added, the packing density of the mix was increased from 0.712 to 0.767, amounting to 8% increase.

Table 2
Packing density and water film thickness of the mortar samples.

Sample no.	Packing density	Excess water ratio	Specific surface area (m^2/m^3)	Water film thickness (μm)
A-0.35		−0.055		−0.076
A-0.40		−0.005		−0.006
A-0.45		0.045	717,900	0.063
A-0.50	0.712	0.095		0.133
A-0.55		0.145		0.202
A-0.60		0.195		0.272
A-0.65		0.245		0.342
B-0.35		−0.037		−0.038
B-0.40		0.013		0.014
B-0.45		0.063		0.065
B-0.50	0.721	0.113	972,100	0.116
B-0.55		0.163		0.168
B-0.60		0.213		0.219
B-0.65		0.263		0.271
C-0.35		−0.013		−0.011
C-0.40		0.037		0.030
C-0.45		0.087		0.071
C-0.50	0.734	0.137	1,226,400	0.112
C-0.55		0.187		0.152
C-0.60		0.237		0.193
C-0.65		0.287		0.234
D-0.35		0.004		0.003
D-0.40		0.054		0.037
D-0.45		0.104		0.071
D-0.50	0.743	0.154	1,480,600	0.104
D-0.55		0.204		0.138
D-0.60		0.254		0.172
D-0.65		0.304		0.206
D-0.70		0.354		0.239
E-0.35		0.030		0.017
E-0.40		0.080		0.046
E-0.45		0.130		0.075
E-0.50	0.757	0.180	1,734,900	0.104
E-0.55		0.230		0.132
E-0.60		0.280		0.161
E-0.65		0.330		0.190
E-0.70		0.380		0.219
F-0.35		0.046		0.023
F-0.40		0.096		0.048
F-0.45		0.146		0.073
F-0.50	0.767	0.196	1,989,100	0.098
F-0.55		0.246		0.123
F-0.60		0.296		0.149
F-0.65		0.346		0.174
F-0.70		0.396		0.199

Note: Sample codes A–F indicate CSF contents of 0%, 5%, 10%, 15%, 20% and 25%, respectively.

The test results in Table 1 showed that when the W/S ratio is relatively low (W/S ratio <0.50), the addition of CSF can increase the flow spread and flow rate, and decrease the yield stress and apparent viscosity. Such improvements in the flowability and rheological properties may be attributed to the increase in the amount of excess water due to the increase in packing density. Although the range of packing density is only about 8%, it has significant effects on the excess water ratio of the mortar, as can be seen from the calculated results for the excess water ratio tabulated in the third column of Table 2. For instance, at the same W/S ratio of 0.35, Mix A-0.35, which has a packing density of 0.712, is calculated to have an excess water ratio of −0.055 (a negative excess water ratio means that the water added was not sufficient to fill up the voids in the mortar leading to the presence of air in the voids), while Mix D-0.35, which has a packing density of 0.743, is calculated to have an excess water ratio of 0.004. With the excess water ratio increased from −0.055 to 0.004 due to the addition of 15% CSF, the flowability and rheological properties of the mortar were significantly improved as evidenced by the increased flow spread and flow rate, and decreased yield stress and apparent viscosity shown in Table 1.

5.2. Solid surface area

Although the addition of CSF up to a CSF content of 25% always increases the packing density and excess water ratio, however, it does not always improve the flowability and rheological properties. The test results in Table 1 show that when the W/S ratio is relatively high (W/S ratio $\geqslant$0.50), the addition of CSF may decrease the flow spread and flow rate, and increase the yield stress and apparent viscosity. For instance, at the same W/S ratio of 0.50, Mix A-0.50 has an excess water ratio of 0.095, while Mix E-0.50 has a higher excess water ratio of 0.180 due to the addition of 20% CSF. Comparing their flowability and rheological properties results in Table 1, it can be seen that despite the significant increase in excess water ratio, the flowability and rheological properties of Mix E-0.50 were not better than those of Mix A-0.50. This may be attributed to the extremely large solid surface area of the CSF particles. The specific surface areas of the six mixes of cementitious materials and fine aggregate area are tabulated in the fourth column of Table 2, where it can be seen that the addition of 20% CSF had increased the specific surface area of the mortar by more than 100%. Hence, the addition of CSF could greatly increase the total solid surface area to be coated by the excess water and thereby significantly reduce the thickness of the water films coating the solid surfaces.

6. Role of water film thickness

From the above, it is evident that the addition of CSF has significant effects on the packing density, excess water ratio, specific surface area and WFT, which in turn govern the flowability and rheological properties of the mortar. The effects of CSF on the packing density and specific surface area are not dependent on the W/S ratio but the effects of CSF on the excess water ratio and WFT are dependent on the W/S ratio. That is the reason why the effects of CSF on the flowability and rheological properties are fairly complicated and dependent on the W/S ratio. Herein, it is suggested that the combined effects of the W/S ratio and CSF content may be evaluated in terms of the WFT, which, to the authors' belief, is the single most important parameter governing the flowability and rheological properties of mortar.

The WFT of the mortar samples, each determined as the respective excess water to solid surface area ratio, are tabulated in the last column of Table 2. For the mortar samples tested, the WFT ranges from −0.076 μm to 0.342 μm. When positive, the WFT has the physical meaning of the average thickness of the water films coating the particles. However, when negative, the WFT no longer has such physical meaning. A negative WFT means that the water added was not sufficient to fill up the voids in the mortar leading to the presence of air in the voids. To better illustrate how the WFT is related to the W/S ratio and CSF content, the WFT is plotted against the CSF content for the different W/S ratios in Fig. 6.

It is noted that the variation of the WFT with the CSF content is dependent on the W/S ratio. At a W/S ratio of 0.35 or 0.40, the WFT increased as the CSF content increased from 0% to 25%, while at a W/S ratio of 0.45, the WFT remained almost unchanged when the CSF content varied. Contrarily, at a W/S ratio of 0.50 or higher, the WFT decreased as the CSF content increased from 0% to 25%. In fact, such changes in WFT are the net effect of the increases in packing density, excess water ratio and specific surface area due to the addition of CSF. Whether the WFT would increase or decrease is dependent on the relative magnitudes of the percentage increase in excess water ratio and the percentage increase in specific surface area. On the whole, the WFT would increase when the percentage increase in excess water ratio is larger than the percentage increase in specific surface area and vice versa.

6.1. Effects of WFT and CSF content on flow spread

By plotting the flow spread against the WFT as shown in the upper half of Fig. 7, it can be seen that in general, the flow spread increased with the WFT at a gradually decreasing rate and that when the WFT was increased to larger than 0.15 μm, the rate of increase in flow spread became so slow that further increase of WFT produced only marginal increase of flow spread. To study the effect of WFT, regression analysis has been carried out to derive the best-fit curve for the flow spread–WFT relation. For easy reference, the best-fit curve so obtained is plotted alongside the data points and its equation and R^2 value are printed in the graph. The coefficient a of the equation of the best-fit curve suggests that the maximum flow spread that can be achieved is about 300 mm. More importantly, the rather low R^2 value of 0.542 indicates that the flow spread is governed not only by the WFT.

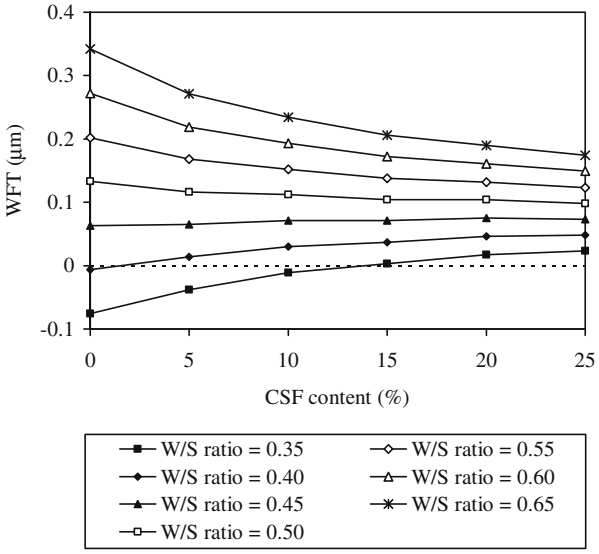

Fig. 6. WFT versus CSF content.

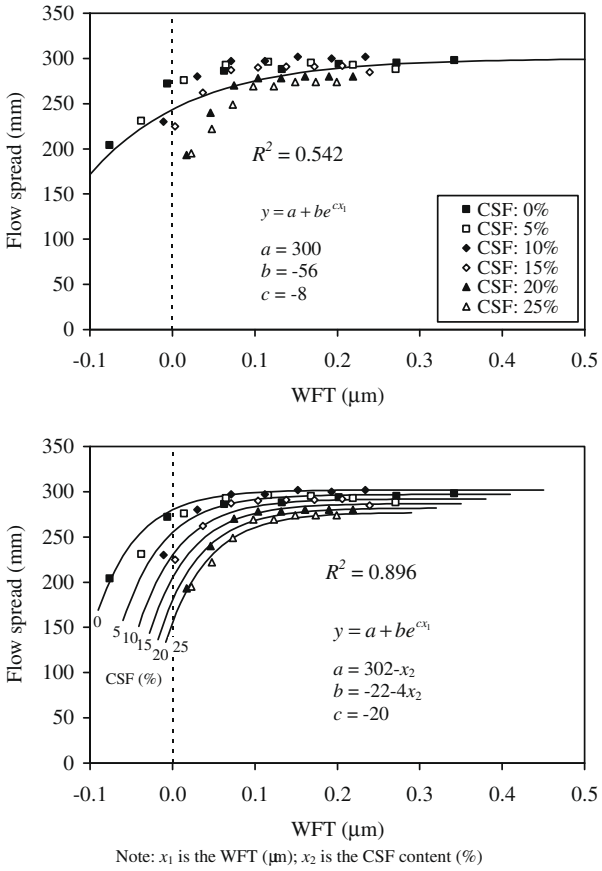

Fig. 7. Flow spread versus WFT.

The data points indeed show that at the same WFT, a mortar having a higher CSF content has a smaller flow spread. Since the effects of CSF on the packing density and solid surface area should have been reflected in the WFT, it seems that the CSF has an additional effect not reflected by the WFT. To study the combined effects of WFT and CSF content, multi-variable regression analysis has been carried out to derive the best-fit curves at different CSF contents, as illustrated in the lower half of Fig. 7. Again, the best-fit curves so obtained are plotted alongside the data points and their equations and R^2 value are printed in the graph. The decreasing value of a with increasing CSF content suggests that the maximum flow spread that can be achieved is lower at a higher CSF content. On the other hand, the much higher R^2 value of 0.896 achieved with both WFT and CSF content considered indicates that the flow spread is governed by both the WFT and CSF content.

The additional effect of CSF not reflected by the WFT is suspected to be caused by the change in cohesiveness of the mortar. When CSF was added, the solid surface area increased and the SP/surface area decreased, leading to increase in electrostatic attractive forces between the solid particles and consequently increase in cohesiveness of the mortar. During the mini slump cone tests, it was observed that at a higher CSF content, the mortar patty formed was generally thicker and more cohesive. Since the volume of mortar sample was constant, the larger thickness of the mortar patty at higher CSF content might have caused the observed smaller flow spread at higher CSF content. To some extent, therefore, the flow spread, as a measure of flowability, is interfered by the cohesiveness of the mortar.

6.2. Effects of WFT and CSF content on flow rate

By plotting the flow rate against the WFT as shown in the upper half of Fig. 8, it can be seen that in general, the flow rate increased with the WFT at a more or less constant rate. To study the effect of WFT, regression analysis has been carried out to derive the best-fit curve for the flow rate–WFT relation. As before, the best-fit curve so obtained is plotted alongside the data points and its equation and R^2 value are printed in the graph. The straight line form of the best-fit curve reveals that the flow rate–WFT relation is basically linear. Furthermore, the very high R^2 value of 0.966 reveals very strong correlation between the flow rate and the WFT.

Despite the high correlation between the flow rate and WFT, it appears that even at a constant WFT, the flow rate varies with the CSF content. To study the combined effects of WFT and CSF content, multi-variable regression analysis has been carried out to derive the best-fit curves at different CSF contents, as illustrated in the lower half of Fig. 8. Again, the best-fit curves so obtained are plotted alongside the data points and their equations and R^2 value are printed in the graph. This time, an even higher R^2 value of 0.988 is achieved. Such an extremely high R^2 value shows very clearly that the flow rate is governed solely by the WFT and CSF content. However, as the CSF content increases, the best-fit curve rotates anticlockwise about a point at WFT = 0.15 μm such that at WFT >0.15 μm, the flow rate would become higher and at WFT <0.15 μm, the flow rate would become lower.

The above phenomenon may be explained as follows. Because of the high fineness, the CSF particles would tend to move together with the water to form a water–CSF slurry. When the WFT is large, the slurry should be quite flowable and would provide lubrication to the cement and aggregate particles. The slurry has a larger volume than the water itself and therefore can increase the spacing between the cement and aggregate particles to reduce their interlocking action. Furthermore, the rounded CSF particles can act as ball bearings to reduce the friction between the cement and aggregate particles. Hence, in such case, the addition of CSF would increase the flow rate of the mortar. On the contrary, when the WFT is small, the water–CSF slurry itself would become very cohesive. At higher CSF content, the cohesiveness is higher due to increase in solid surface area and decrease in SP/surface area. As a result, the water–CSF slurry would become less effective in lubricating the cement and aggregate particles. Furthermore, as the CSF particles themselves would not easily roll over each other due to the small WFT, they might no longer be able to act as ball bearings. Hence, in such case, the addition of CSF would decrease the flow rate of the mortar.

6.3. Effects of WFT and CSF content on yield stress

The yield stress is plotted against the WFT in Fig. 9 to illustrate the effect of WFT on yield stress. In general, the yield stress decreased as the WFT increased. This phenomenon is expected since a water–solid mixture with a larger WFT should require a smaller shear stress to flow. To study the effect of WFT, regression analysis has been carried out to derive the best-fit curve for the yield stress–WFT relation. The best-fit curve so obtained and its equation and R^2 value are presented in the graph for easy reference. A fairly good R^2 value of 0.847 has been achieved, indicating that the yield stress is dependent mainly on the WFT. Nevertheless, it still appears that when the WFT is smaller than 0.15 μm, the yield stress is dependent not only on the WFT but also on the CSF content.

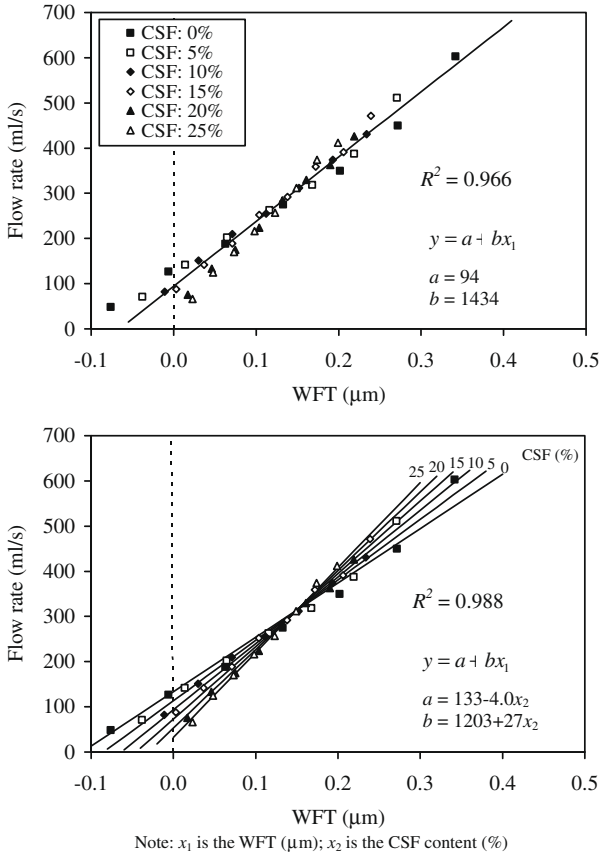

Fig. 8. Flow rate versus WFT.

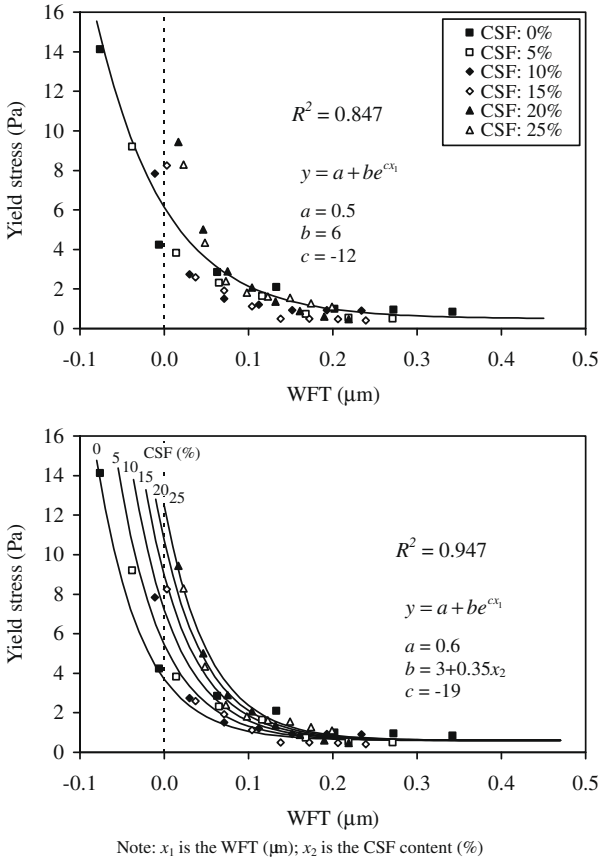

Fig. 9. Yield stress versus WFT.

To study the combined effects of WFT and CSF content, multi-variable regression analysis has been carried out to derive the best-fit curves at different CSF contents, as illustrated in the lower half of Fig. 9. The best-fit curves so obtained are plotted alongside the data points and their equations and R^2 value are printed in the graph. It is noted that as the CSF content increases, the best-fit curve shifts to the right. Such shifting reveals that at small WFT, the yield stress would increase with the CSF content while at large WFT, the yield stress is dependent solely on the WFT. This may be explained by the fact that when the WFT is small, a mortar containing more CSF would have a higher cohesiveness (due to increase in solid surface area and decrease in SP/surface area) and thus require a higher shear stress to flow. Lastly, it is noteworthy that with both the WFT and CSF content considered in the correlation, the R^2 value is increased to a very high value of 0.947.

6.4. Effects of WFT and CSF content on apparent viscosity

The apparent viscosity is plotted against the WFT in Fig. 10 to illustrate the effect of WFT on apparent viscosity. As for the yield stress, the apparent viscosity decreased as the WFT increased. To study the effect of WFT, regression analysis has been carried out to derive the best-fit curve for the apparent viscosity–WFT relation. The best-fit curve so obtained and its equation and R^2 value are presented in the graph for easy reference. A fairly good R^2 value of 0.857 has been achieved, indicating that the apparent viscosity is dependent mainly on the WFT. Nevertheless, it still appears that when the WFT is smaller than 0.15 μm, the apparent viscosity is dependent not only on the WFT but also on the CSF content.

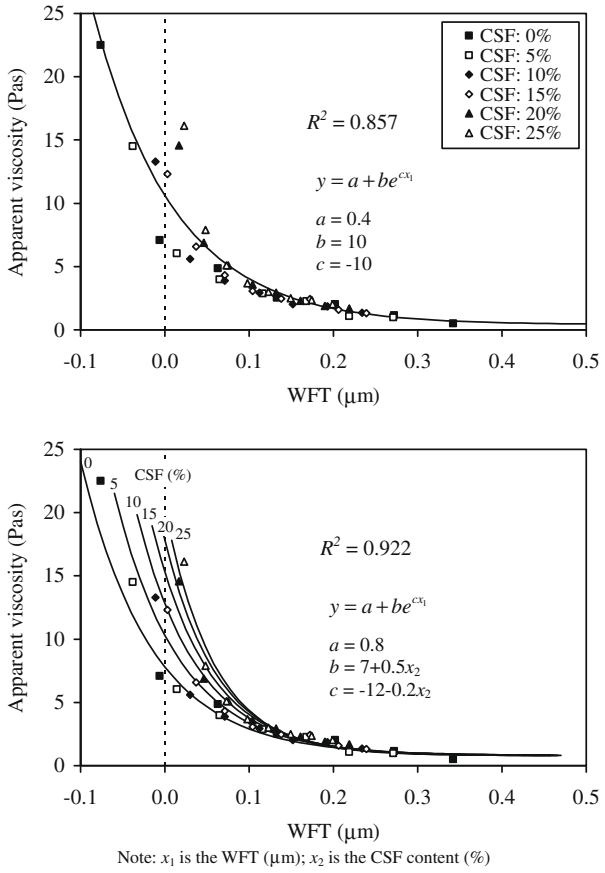

Note: x_1 is the WFT (μm); x_2 is the CSF content (%)

Fig. 10. Apparent viscosity versus WFT.

As before, multi-variable regression analysis has been carried out to evaluate the combined effects of WFT and CSF content. The best-fit curves at different CSF contents and their equations and R^2 value are presented alongside the data points in the lower half of Fig. 10. It is seen that as the CSF content increases, the best-fit curve would shift to the right. Such shifting of the best-fit curve reveals that at small WFT, the apparent viscosity would increase with the CSF content while at large WFT, the apparent viscosity is dependent solely on the WFT. The cause of such increase in apparent viscosity with the CSF content at small WFT should be the same as that of the increase in yield stress with the CSF content at small WFT, as explained before. With both the WFT and CSF content considered in the correlation, the R^2 value is increased to a very high value of 0.922.

7. Conclusions

A total of 45 mortar samples proportioned with different CSF contents and different W/S ratios were produced for packing density, flowability and rheological properties measurements. For the packing density measurement, the wet packing test recently developed by the authors' research group was applied. On the other hand, the flowability was measured by the mini slump cone and mini V-funnel tests whereas the rheological properties were measured by the vane test using a rheometer. On the whole, the test results revealed that both the W/S ratio and CSF content have major effects on the flowability and rheological properties of mortar. As expected, the flowability and rheological properties always improved as the W/S ratio increased. However, the effects of CSF content appeared to be fairly complicated.

In-depth analysis showed that the effects of CSF content are dependent on the W/S ratio. When the W/S ratio <0.50, there is an optimum CSF content at which the flowability is highest and the yield stress and apparent viscosity are lowest. When the W/S ratio $\geqslant$0.50, both the flowability and rheological properties are impaired by the addition of CSF. At the same time, the addition of CSF up to 25% by volume would lead to an increase in packing density, which should be beneficial, and an increase in solid surface area, which could be detrimental. From the packing density and solid surface area results, the WFT of each mortar sample was evaluated and its effects on the flowability and rheological properties of mortar were studied. Correlations of the flow spread, flow rate, yield stress and apparent viscosity to the WFT yielded R^2 values of 0.542, 0.966, 0.847 and 0.857, respectively. Hence, despite complications caused by the presence of CSF, the WFT is still the single most important parameter governing the flowability and rheological properties of CSF mortar.

In some cases, however, it was found that even at the same WFT, the flowability and rheological properties varied significantly with the CSF content. This suggested that although the effects of CSF on packing density and solid surface area should have been reflected in the WFT, there is an additional effect of CSF not reflected by the WFT. To study the combined effects of WFT and CSF content, multi-variable regression analysis has been carried out. Correlations of the flow spread, flow rate, yield stress and apparent viscosity to both the WFT and CSF content yielded R^2 values of 0.896, 0.988, 0.947 and 0.922, respectively. The much better correlations obtained proved that the flowability and rheological properties of CSF mortars are dependent not only on the WFT but also on other factors related to the presence of CSF. It is suspected that the increased cohesiveness due to increase in solid surface area and decrease in SP/surface area, the lubrication effects of the water–CSF slurry and the ball bearing effect of the CSF particles might also be playing certain roles in the rheology of CSF mortar. Further research is highly recommended.

Acknowledgement

The work described in this paper was fully supported by a Grant from the Research Grants Council of the Hong Kong Special Administrative Region, China (Project No. 713309).

References

[1] Khatri RP, Sirivivatnanon V, Gross W. Effect of different supplementary cementitious materials on mechanical properties of high performance concrete. Cem Concr Res 1995;25(1):209–20.
[2] Aïtcin PC. High-performance concrete. London: E&FN Spon; 1998. p. 139–56.
[3] Rizwan SA, Bier TA. Self-consolidating mortars using various secondary raw materials. ACI Mater J 2009;106(1):25–32.
[4] Gesoğlu M, Güneyisi E, Özbay E. Properties of self-compacting concretes made with binary, ternary, and quaternary cementitious blends of fly ash, blast furnace slag, and silica fume. Constr Build Mater 2009;23(5):1847–54.
[5] Malhotra VM, Ramachandran VS, Feldman RF, Aïtcin PC. Condensed silica fume. Florida: CRC Press; 1987. p. 1–5.
[6] Wolsiefer J. Ultra high-strength field placeable concrete with silica fume admixture. Concr Int 1984;6(4):25–31.
[7] Hooton RD. Influence of silica fume replacement of cement on physical properties and resistance to sulfate attack, freezing and thawing, and alkali-silica reactivity. ACI Mater J 1993;90(2):143–51.
[8] Bayasi Z, Zhou J. Properties of silica fume concrete and mortar. ACI Mater J 1993;90(4):349–56.
[9] Alexander MG, Magee BJ. Durability performance of concrete containing condensed silica fume. Cem Concr Res 1999;29(6):917–22.
[10] Mazloom M, Ramezanianpour AA, Brooks JJ. Effect of silica fume on mechanical properties of high-strength concrete. Cem Concr Compos 2004;26(4):347–57.
[11] Kohno K, Komatsu H. Use of ground bottom ash and silica fume in mortar and concrete. In: Malhotra VM, editor. Proceedings of the ACI second international conference on fly ash, silica fume, slag, and natural pozzolans in concrete: ACI SP 91. Madrid, Spain: American Concrete Institute; 1986. p. 1279–92.
[12] Duval R, Kadri EH. Influence of silica fume on the workability and the compressive strength of high-performance concretes. Cem Concr Res 1998;28(4):533–47.
[13] Zhang X, Han J. The effect of ultra-fine admixture on the rheological property of cement paste. Cem Concr Res 2000;30(5):827–30.
[14] Artelt C, Garcia E. Impact of superplasticizer concentration and of ultra-fine particles on the rheological behaviour of dense mortar suspensions. Cem Concr Res 2008;38(5):633–42.
[15] Helmuth RA. Structure and rheology of fresh cement paste. In: Proceedings of 7th international congress of chemistry of cement: sub-theme VI-0; 1980. p. 16–30.
[16] Zhang C, Wang A, Tang M, Liu X. The filling role of pozzolanic material. Cem Concr Res 1996;26(6):943–7.
[17] Nanthagopalan P, Haist M, Santhanam M, Müller HS. Investigation on the influence of granular packing on the flow properties of cementitious suspensions. Cem Concr Compos 2008;30(9):763–8.
[18] Peng Y, Hu S, Ding Q. Dense packing properties of mineral admixtures in cementitious material. Particuology 2009;7(5):399–402.
[19] Wong HHC, Kwan AKH. Packing density of cementitious materials: part 1–measurement using a wet packing method. Mater Struct 2008;41(4):689–701.
[20] Fung WWS, Kwan AKH, Wong HHC. Wet packing of crushed rock fine aggregate. Mater Struct 2009;42(5):631–43.
[21] Kwan AKH, Fung WWS. Packing density measurement and modelling of fine aggregate and mortar. Cem Concr Compos 2009;31(6):349–57.
[22] Wong HHC, Kwan AKH. Packing density of cementitious materials: measurement and modelling. Mag Concr Res 2008;60(3):165–75.
[23] Kwan AKH, Wong HHC. Effects of packing density, excess water and solid surface area on flowability of cement paste. Adv Cem Res 2008;20(1):1–11.
[24] Wong HHC, Kwan AKH. Rheology of cement paste: role of excess water to solid surface area ratio. J Mater Civ Eng 2008;20(2):189–97.
[25] Kwan AKH, Fung WWS, Wong HHC. Water film thickness, flowability and rheology of cement–sand mortar. Adv Cem Res 2010;22(1):3–14.
[26] Okamura H, Ouchi M. Self-compacting concrete. J Adv Concr Technol 2003;1(1):5–15.